Monitoring Neural Activity with Bioluminescence during Natural Behavior

E. A. Naumann*, A. R. Kampff*, D. A. Prober, A. F. Schier and F. Engert

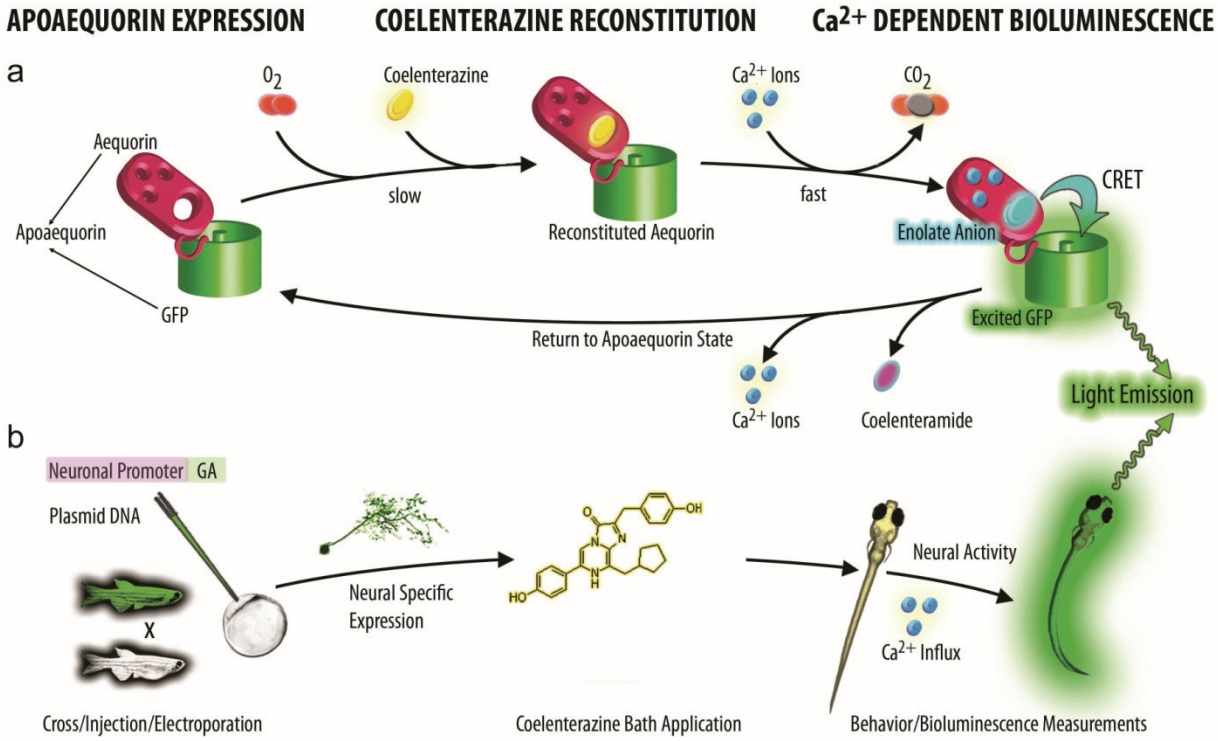

Supplementary Figure 1 – Neuroluminescence in zebrafish: mechanism and method

The upper diagram (**a**) schematizes the molecular reaction underlying the Ca^{2+}-dependent light emission of GFP-Aequorin (GA) and the lower diagram (**b**) demonstrates how GA was employed as a bioluminescence reporter of neural activity in freely swimming zebrafish. **a** Light emission first requires the reaction of GFP-apoAequorin (Ga) with coelenterazine. After reacting with oxygen to form a stable peroxide intermediate, a coelenterazine molecule will stably bind to Ga to form GA. In this reconstituted form, the binding of Ca^{2+} ions induces a conformational change in GA that initiates the oxidative decarboxylation of coelenterazine, releasing CO_2 and producing an excited enolate anion. By a process known as non radiative chemiluminescent resonance energy transfer (CRET), the energy from the excited anion is transferred to GFP and results in the emission of a green photon. After photon emission, both the coelenteramide and Ca^{2+} are released and Ga is again available for reconstitution. **b** Neural expression of Ga is achieved by microinjecting embryos at the single-cell stage with plasmid DNA encoding Ga under control of a neuron specific promoter. Generation of stable transgenic fish or other expression targeting methods (e.g. electroporation) can also be used to introduce Ga into neurons of interest. Neuronal Ga is exposed to coelenterazine *in* vivo, in order to form the luminescent GA, by immersing the entire zebrafish larva in embryo medium containing coelenterazine dissolved in cyclodextrin. After an incubation time, neural Ca^{2+}-dependent light emission, neuroluminescence, can be detected during unrestrained behavior.

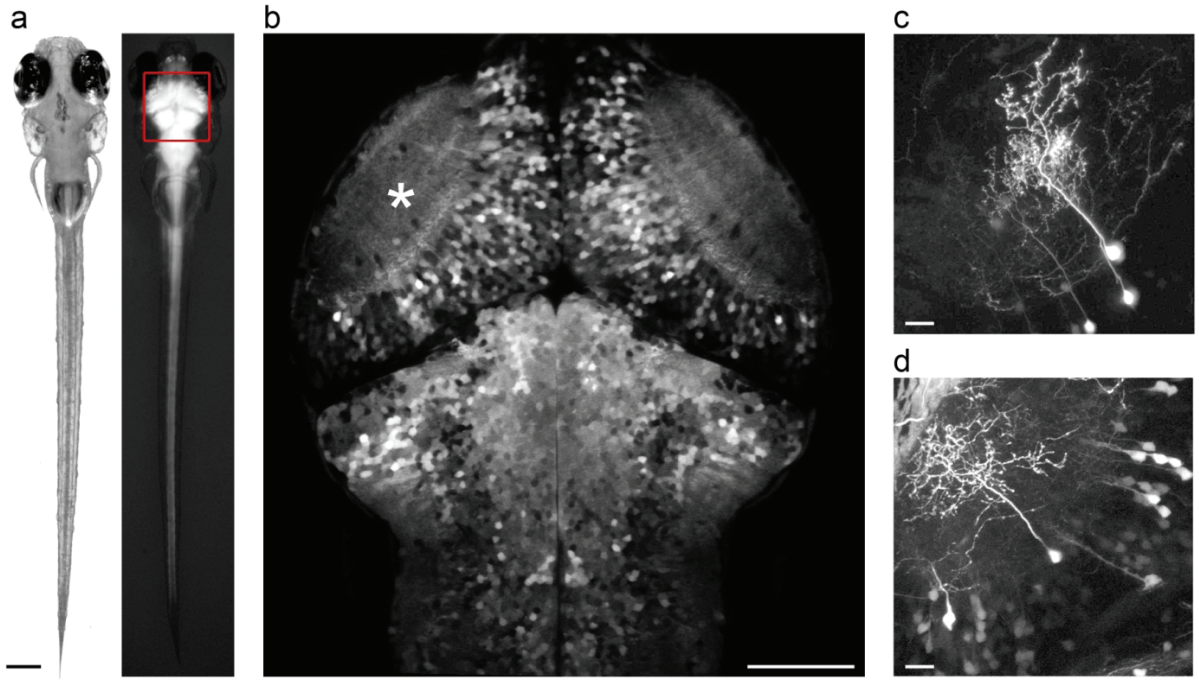

Supplementary Figure 2 – Neural specific expression of GFP-Aequorin (Ga)

a Bright field and fluorescence micrographs of a 7 dpf transgenic NβT:Ga larval zebrafish (scale bar: 0.2 mm). **b** A two-photon optical section through the dorsal midbrain and hindbrain (scale bar: 100 µm). **c-d** Two-photon maximum intensity z-projections of the left optic tectum in two zebrafish larvae that transiently expressed Ga following plasmid injection at the single-cell stage. The *neural-β-tubulin* promoter specifically targets Ga expression to neurons, which appear healthy during all observed developmental stages (3-10 dpf) (scale bar: 20 µm).**c** Mosaic expression of Ga with *neural-β-tubulin:Ga* (6 dpf).**d** Expression of Ga by co-injection of plasmids encoding *neural-β-tubulin:Gal4* and *UAS:Ga,* demonstrating that a binary expression system can be used to target Ga expression to specific neurons (6 dpf).

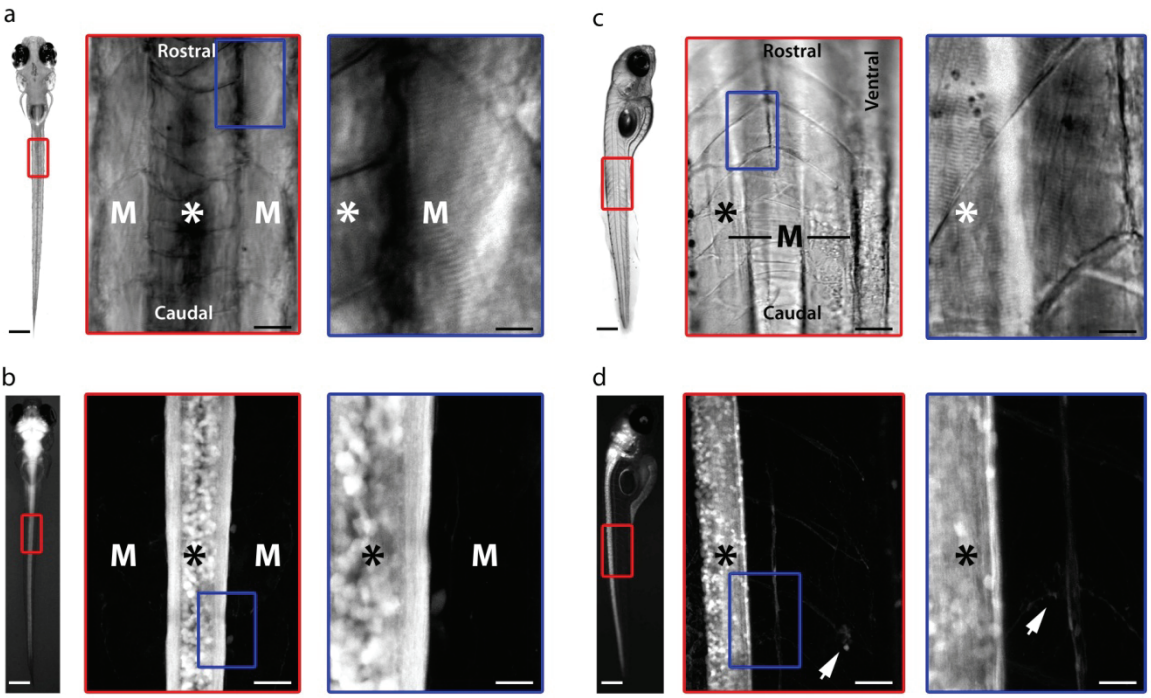

Supplementary Figure 3 – Neural specific expression of GFP-Aequorin (Ga) in the Zebrafish Tail
a (left) Dorsal bright field micrograph of a 7 dpf zebrafish (scale bar: 0.3 mm). (middle) An expanded view of the region indicated (red rectangle) focusing on the tail of the fish. Neurons of the spinal cord (*) are located along the midline above the notochord. Axial musculature surrounds the fish tail. Epaxial muscles are not easily visible on the dorsal side, but the lateral hypaxial muscles (M), and the segregated myotomes, are clearly visible (scale bar: 50 µm). (right) A higher magnification image of the indicated region (blue rectangle) reveals the dark stripes characteristic of the sarcomeres of skeletal muscles (M) (scale bar: 20 µm). **b** (left) Dorsal bright field and fluorescence micrograph of a 7 dpf transgenic Nβt:Ga zebrafish (scale bar: 0.3 mm). The indicated region (red rectangle) shows the position of subsequent two-photon investigation of Ga expression. (middle) A maximum intensity projection of a series of images acquired with a two-photon microscope through the complete depth, 370 µm, of the tail (scale bar: 50 µm). Specific neural expression in spinal cord neurons and lateral axon tracks (*) can be seen in the center; a few neural processes and auto-fluorescence from skin is detected in the region overlapping with the lateral hypaxial muscles (M). (right) A zoom-in on the indicated region (blue rectangle) further demonstrates that Ga expression is only detected in neuronal structures (scale bar: 20 µm). **c** (left) Lateral bright field micrograph of a 7 dpf zebrafish (scale bar: 0.3 mm). (middle) An expanded view of the region indicated (red rectangle) focusing on the tail of the fish. Neurons (*) of the spinal cord are positioned dorsal to the notochord. The segregated myotomes of the axial musculature that surrounds the fish (M) can be seen (scale bar: 50 µm). (right) A higher magnification of the indicated region (blue rectangle) also reveals dark stripes characteristic of the sarcomeres of skeletal muscles (M) and the location of the spinal cord track(*)

(scale bar: 20 μm). **d** (left) Lateral bright field and fluorescence micrograph of a 7 dpf transgenic Nβt:Ga zebrafish (scale bar: 0.3 mm). The indicated region (red rectangle) shows the position of subsequent two-photon investigation of Ga expression. (middle) A maximum intensity projection of a series of images acquired with a two-photon microscope through the complete depth, 250 μm, of the tail (scale bar: 50 μm). Specific neural expression in spinal cord is apparent; only neural processes and auto-fluorescence from skin is observed in the region overlapping with the axial muscles (M). (right) A zoom-in on the indicated region (blue rectangle) further demonstrates that Ga expression is only detected in neuronal structures (scale bar: 20 μm). Arrows indicate neural processes innervating the musculature.

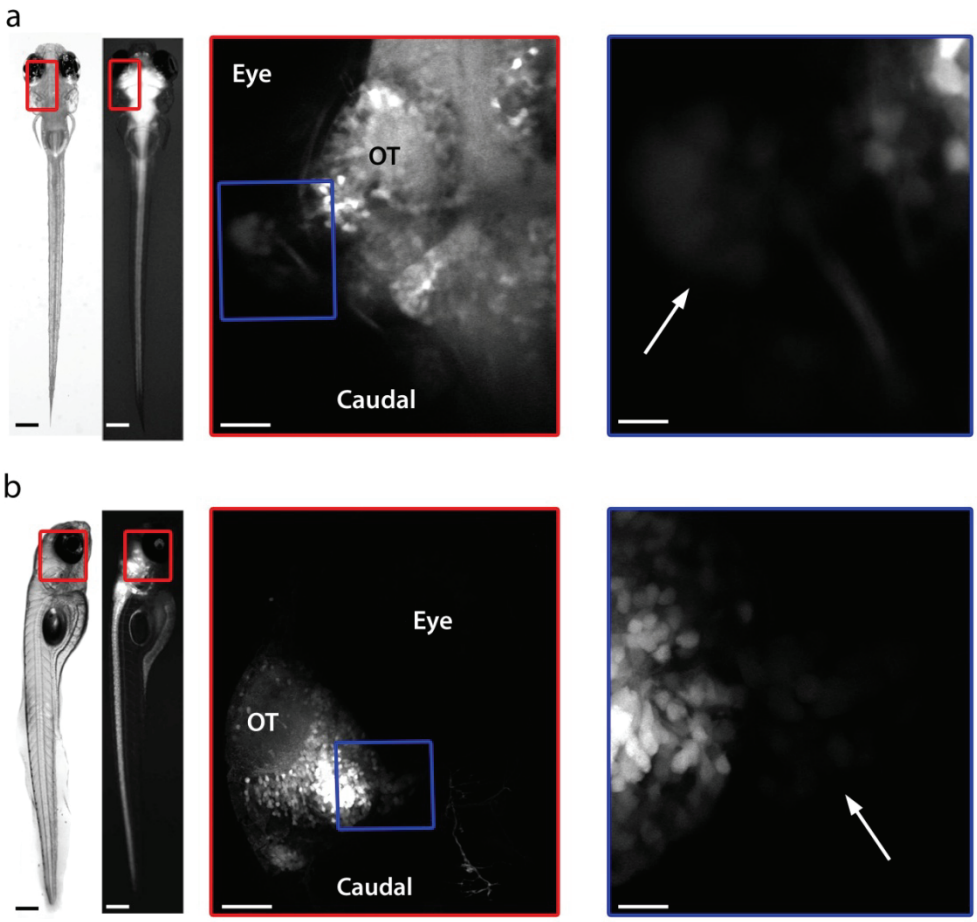

Supplementary Figure 4 – Neural specific expression of GFP-Aequorin (Ga) in Trigeminal Neurons
a (left) Dorsal bright field and fluorescence micrographs of a 7 dpf transgenic Nβt:Ga zebrafish (scale bar: 0.3 mm). Rectangle indicates the region imaged with two-photon microscopy. (middle) A maximum intensity projection through the ventral portion of the left optic tectum (OT) and trigeminal nucleus (scale bar: 50 µm). (right) A higher magnification image of the indicated region (blue rectangle) reveals the low expression level of Ga in trigeminal neurons (arrow) compared to other neurons of the zebrafish brain (scale bar: 20 µm). **b** (left) Lateral bright field and fluorescence micrographs of a 7 dpf transgenic Nβt:Ga zebrafish (scale bar: 0.3 mm). Rectangle indicates the region imaged with two-photon microscopy. (middle) A maximum intensity projection of sagittal sections through the right optic tectum (OT) and trigeminal nucleus (scale bar: 50 µm). (right) A higher magnification image of the indicated region (blue rectangle) again reveals the low expression level of Ga in trigeminal neurons (arrow) compared to the more dorsal neurons of the zebrafish brain (scale bar: 20 µm). Note that only neural structures are visible, even though expression level varies, and that there is no detectable expression in regions where facial and axial muscles are located.

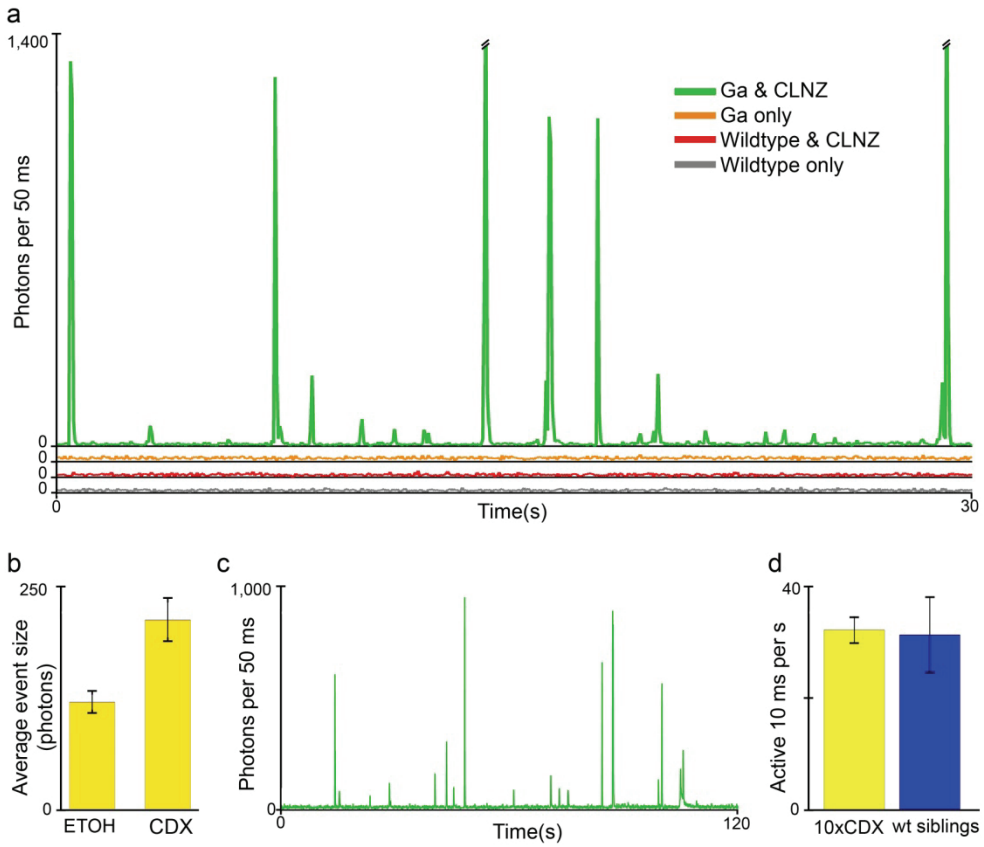

Supplementary Figure 5 – Reconstitution of Aequorin with coelenterazine

a Total light emission produced by groups of five 5-6 dpf larvae representing different Ga and coelenterazine (CLZN) combinations. Neuroluminescence is only detected from Ga transgenic zebrafish after soaking in embryo medium containing 40 µM coelenterazine (Ga & CLZN), suggesting that detected photons were generated by reconstituted Aequorin. Ga transgenic zebrafish raised in normal embryo medium (Ga only), *nacre* wild-type zebrafish soaked in normal embryo medium (wildtype only) or *nacre* wild-type zebrafish soaked in embryo medium containing 40 µM coelenterazine (wildtype & CLZN) show no photon emission. The low number of photon events detected for the other conditions arise from dark counts generated at the PMT photocathode. The Y-axis for each experimental group is offset by 25 counts to facilitate comparison between the different conditions. **b** The average number of photons within the transient neuroluminescent events produced by GA in zebrafish exposed to CLZN dissolved in ethanol or cyclodextrin are shown. Fish were tested in groups of 5 (n = 30) for 10 minutes (error bars represent s.e.m.). **c** Cyclodextrin-dissolved coelenterazine is able to reconstitute Aequorin and sustain neuroluminescence until at least 11 dpf (a two minute recording from an 11 dpf GA zebrafish shown). The coelenterazine bath solution was replaced every 2 days. **d** Wild-type zebrafish were exposed to a ten-fold higher concentration (400 µM) of Cyclodextrin (CDX) without coelenterazine from 3 dpf to 5 dpf and tested for behavioral activity (the number of 10 ms periods in which motion was detected per second). When compared to untreated siblings (fish were tested in groups of 5 with a total of 80 fish in each condition), no difference in activity level was observed (error bars represent s.e.m.).

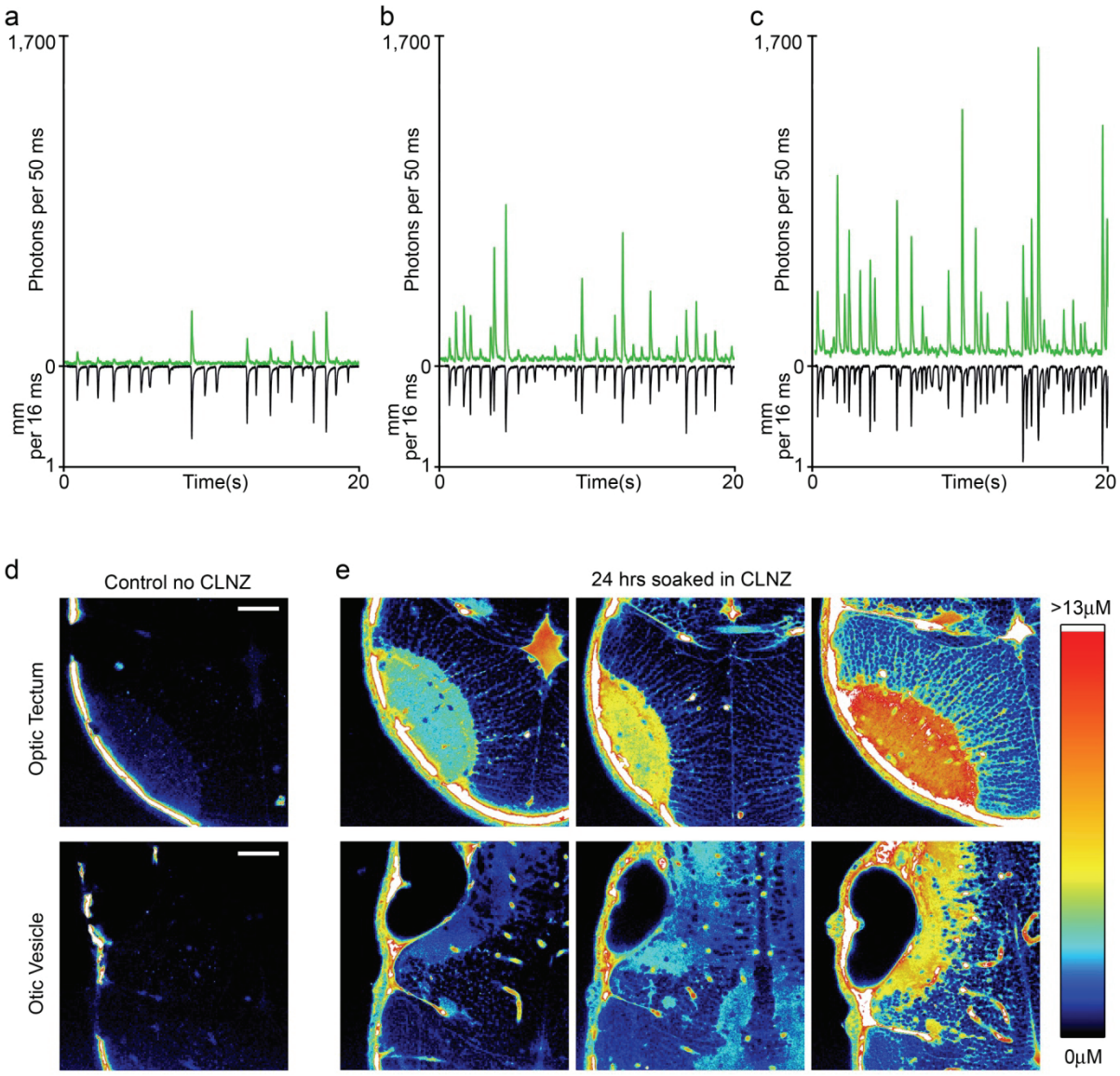

Supplementary Figure 6 – Variation in signal amplitude and coelenterazine loading

a-c Neuroluminescence signals produced by three 6 dpf zebrafish siblings and their corresponding swim velocity (mm/frame period (16.67 ms)). Each sibling was exposed to CLZN-*h* for 24 hours under identical conditions (in the same rearing dish). Neuroluminescence corresponding to behavioral events can be detected in all 3 individuals; however, the peak signal amplitudes vary from fish to fish. For the fish shown in **a**, small neuroluminescence events are visible, but almost no baseline neuroluminescence is detectable, whereas the fish in **b** and **c** show not only larger transient neuroluminescence signals, but also an increase in the baseline neuroluminescence which possibly reflects a corresponding increase in background neural activity. **d-e** Two-photon horizontal sections through the optic tectum and the otic vesicle comparing the amount of CLZN-fluorescence in 4 dpf non-transgenic *nacre* zebrafish (scale bar: 40 µm). A control zebrafish not exposed to CLZN exhibits strong auto-fluorescence from the skin, but weak auto-fluorescence

within the brain. **e** Individual larvae exposed to CLZN 24 hours prior to imaging exhibit strong fluorescence in neural tissue resulting from the excitation of CLZN that was absorbed into the brain. Each image is color coded according to reflect the calibrated CLZN concentration (see gradient scale). Weak signal in cell body regions could be caused by exclusion of CLZN from the nucleus of neurons, however, CLZN is clearly detected within the brain of each larva and the observed differences in concentration may explain some of the observed variability in peak neuroluminescence signals.

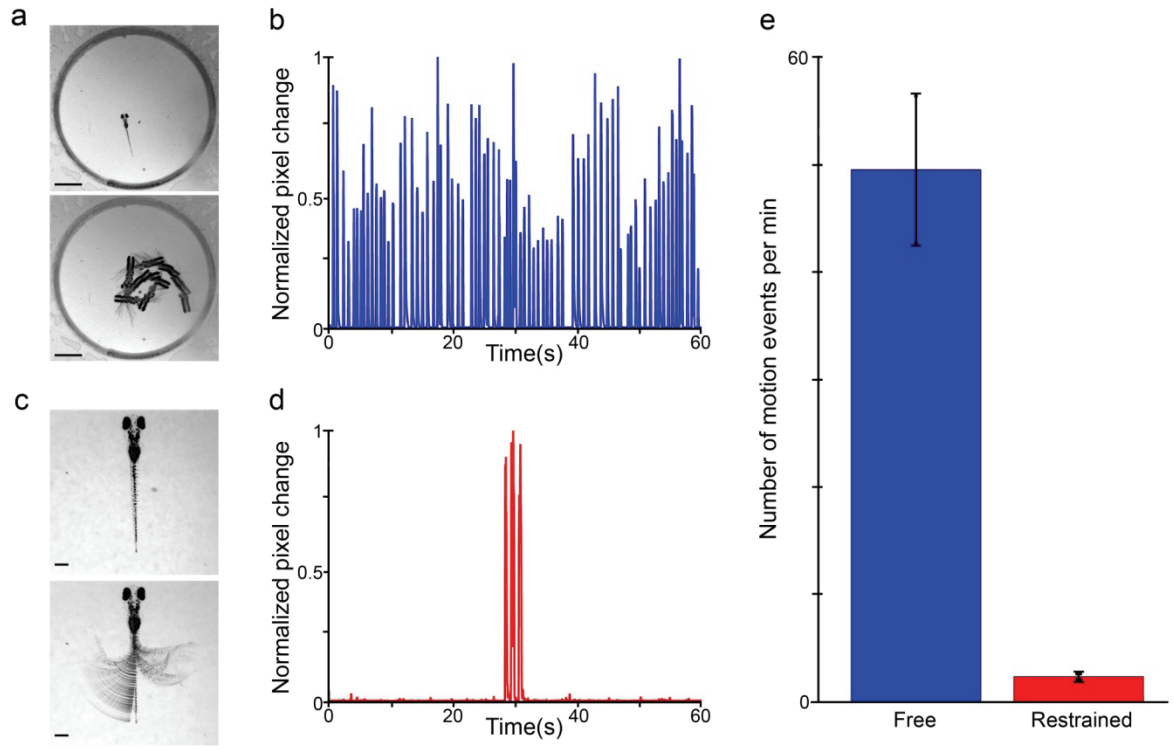

Supplementary Figure 7 – Restraining zebrafish substantially reduces spontaneous activity
a A single image of a freely swimming zebrafish (top) and the minimum intensity projection of a 3 second image sequence (bottom) (scale bar: 2.5 mm). **b** The activity of a 6 dpf fish, measured as the frame to frame pixel change (acquired at 50 Hz) normalized to the maximum value, is plotted for a 60 second time period. Each peak in the activity recording, which corresponds to a discrete swim bout, is counted as a single motion event. **c** A single image of a partially restrained zebrafish (top), and a maximum intensity projection of a 3 second image sequence (bottom) during a bout of spontaneous behavior (scale bar: 0.35 mm). The fish's head is embedded in low melting agarose, but the tail is free to move. **d** The activity of a head-restrained 6 dpf fish, measured as the frame to frame pixel change (acquired at 50 Hz) normalized to the maximum value, is plotted for a 60 second time period. Each peak in the activity recording, which corresponds to a discrete bout of tail motion, is counted as a single motion event. Note that a complete lack of activity in the restrained fish is interrupted by a brief burst of struggle-like bouts of tail motion. **e** A comparison of the mean number of spontaneous motion events per minute in free versus head-restrained zebrafish reveals a dramatic reduction in spontaneous activity during restraint (n = 10 zebrafish in each group, 5-6 dpf, error bars represent s.e.m.).

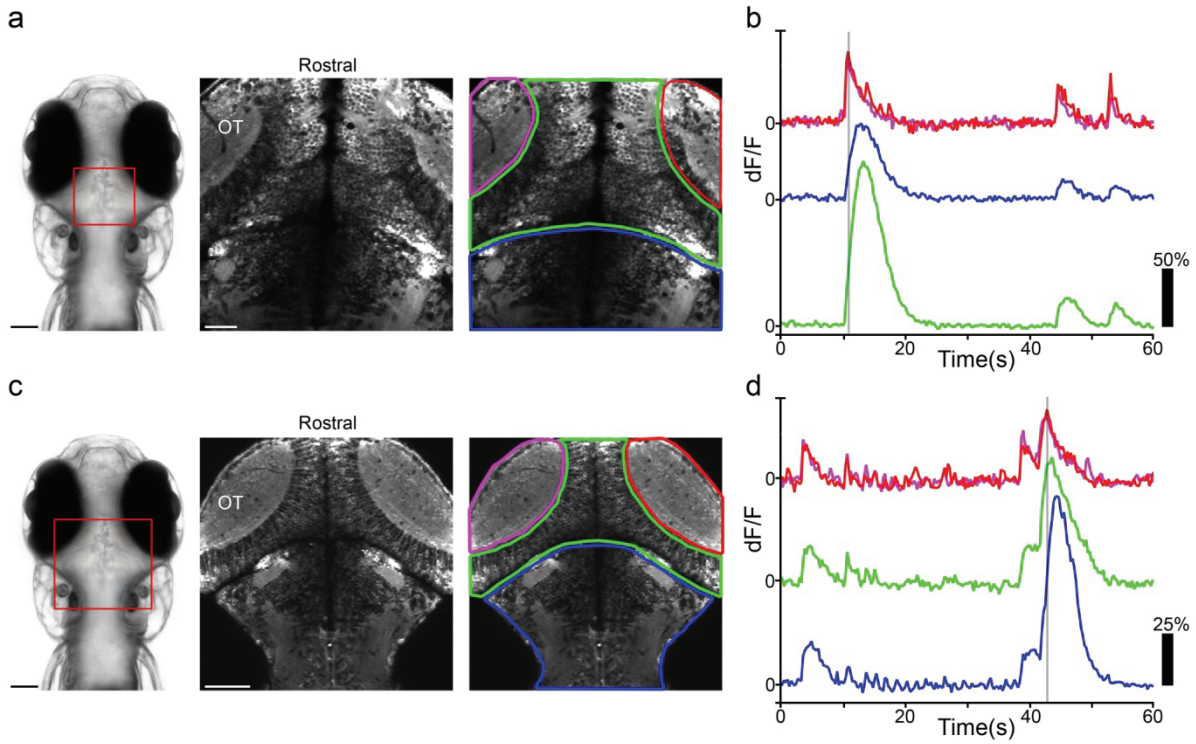

Supplementary Figure 8 – PTZ evoked calcium responses in HuC:GCaMP2 transgenic zebrafish
a (left) Dorsal bright field micrograph of a 7 dpf zebrafish (scale bar: 0.15 mm). The rectangle indicates the region selected for calcium imaging. (middle) A HuC:GCaMP2 zebrafish was embedded in low melting agarose, paralyzed, and imaged with a two-photon microscope. The average intensity image of the acquired time-series reveals expression of GCaMP2 in the optic tectum (OT), midbrain, and hindbrain of this transgenic zebrafish (scale bar: 50 µm). (right) Regions of interest within the right and left tectal neuropils, midbrain somatic region, and hindbrain are shown; these regions were used in analysis of the calcium-dependent fluorescence signal. **b** During PTZ exposure, sporadic waves of correlated activity were detected throughout the zebrafish brain. The integrated δF/F (%) signals from each region are shown in the corresponding color; a vertical line aligned to the earliest signal peak (in the tectal neuropil) is shown to facilitate comparison of the peak signal times in the different brain regions. These transient responses have time courses comparable to the sustained neuroluminescence events observed in paralyzed Nβt:GA zebrafish (**Figure 3j**). **c-d** An additional example of the experiment described in **a-b** in which a larger, more dorsal plane of the zebrafish brain was investigated. **c** (middle image, scale bar: 100 µm) **d** Unlike in **b**, the hindbrain is the final region to reach peak signal intensity.

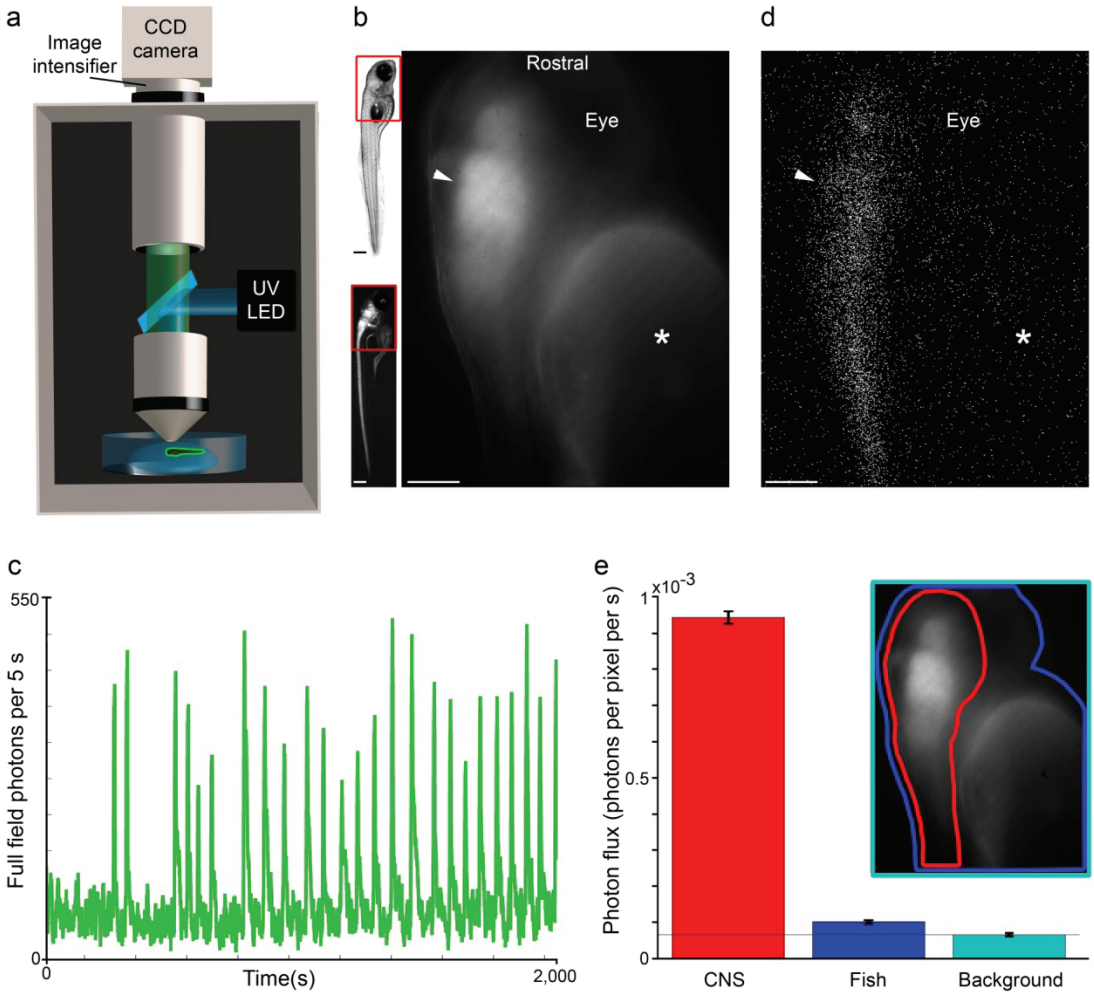

Supplementary Figure 9 – Photons are generated by neural structures in Nβt:GA transgenic fish

a Schematic diagram of photon-counting imaging apparatus: an intensified CCD camera, custom epi-fluorescence microscope, and excitation light (UV LED) are assembled within a light tight enclosure. **b** A 5 dpf Nβt:GA larva was immobilized on its side in low melting point agarose and the rectangle overlay indicates the region imaged to localize Aequorin expression via GFP fluorescence. The arrow indicates the dorsal portion of the zebrafish brain and the auto-fluorescent swim bladder is indicated with a star symbol (*) (scale bar: 100 μm). **c** When epileptic-like neural activity is induced by the addition of PTZ (10 mM), transient increases in the total number of photons were observed . **d** The positional origin of the detected photons during these transient events is plotted. Also in a non-paralyzed zebrafish, the majority of photons arrive from the region containing neurons of the brain and spinal cord (CNS); arrow and start symbol (*) are located at the same position as in **b** (scale bar: 100 μm). **e** The photon flux (photons/pixel/second) from within three regions of interests (see inset): CNS, the imaged portion of the zebrafish excluding the CNS, and the background (error bars represent s.e.m.). Photon flux from the non-neuronal region of the zebrafish is slightly above the background dark counts, which could result from photons that originate from neurons being scattered by the fish body tissue or from neural processes located throughout the fish.

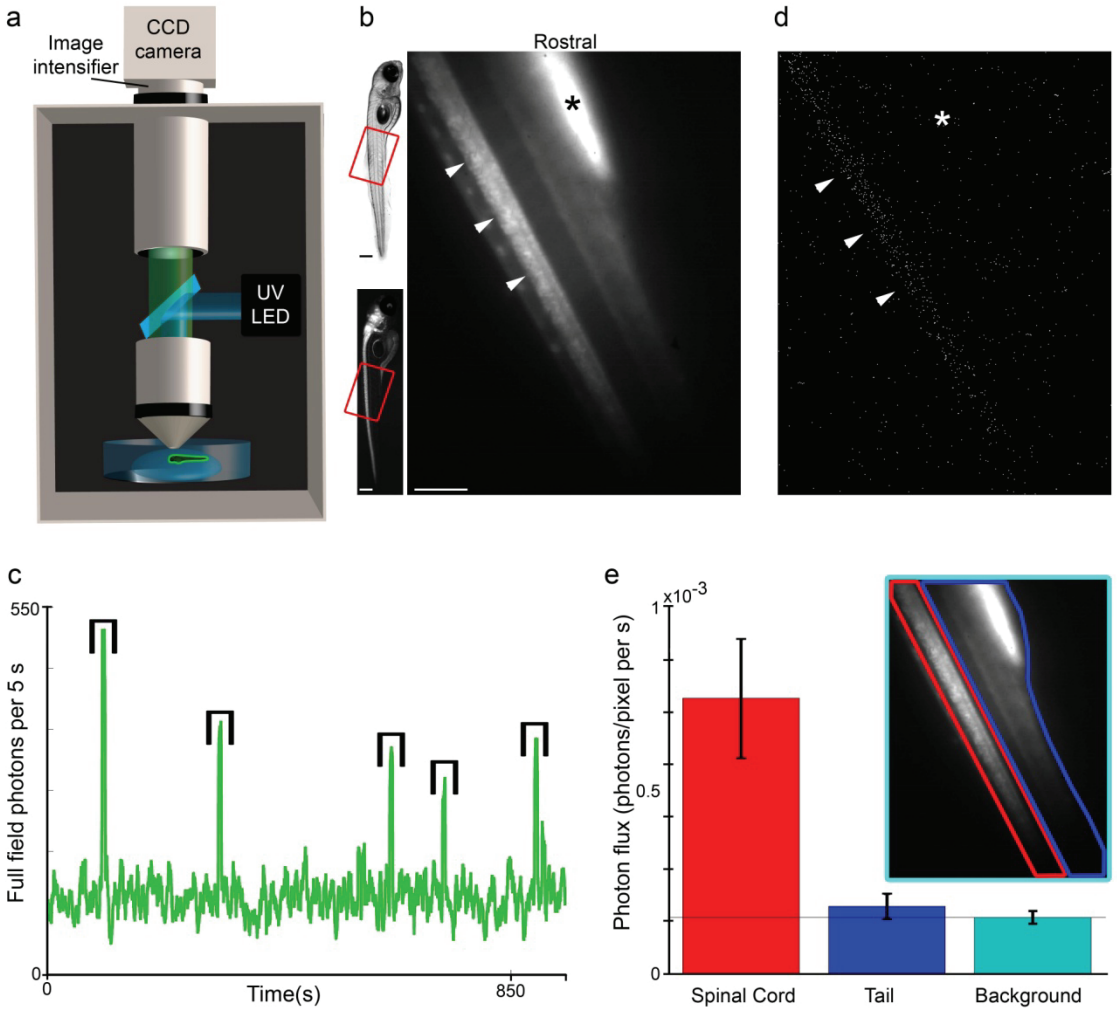

Supplementary Figure 10 – Photons are generated by neural structures in the spinal cord

a Schematic diagram of photon-counting imaging apparatus: an intensified CCD camera, custom epi-fluorescence microscope, and excitation light (UV LED) are assembled within a light tight enclosure. **b** A 5 dpf Nβt:GA larva was immobilized on its side in low melting point agarose and the rectangle overlay indicates the region imaged to localize Aequorin expression via GFP fluorescence. The arrows indicate regions of the spinal cord and the auto-fluorescent swim bladder is indicated with a star symbol (*) (scale bar: 100 μm). **c** When epileptic-like neural activity is induced by the addition of PTZ (10 mM), transient increases in the total number of photons were observed . **d** The positional origin of the detected photons during these transient events is plotted. The majority of photons arrive from the region containing neurons of the spinal cord; arrows and star symbol (*) are located at the same position as in **b**. **e** The photon flux (photons/pixel/second) from within three regions of interests (see inset): spinal cord, the imaged portion of the zebrafish excluding the spinal cord, and the background (error bars represent s.e.m.). Photon flux from the non-neuronal region of the zebrafish is slightly above the background dark counts, which could result from photons that originate from neurons being scattered by the fish body tissue or from neural processes located throughout the fish.

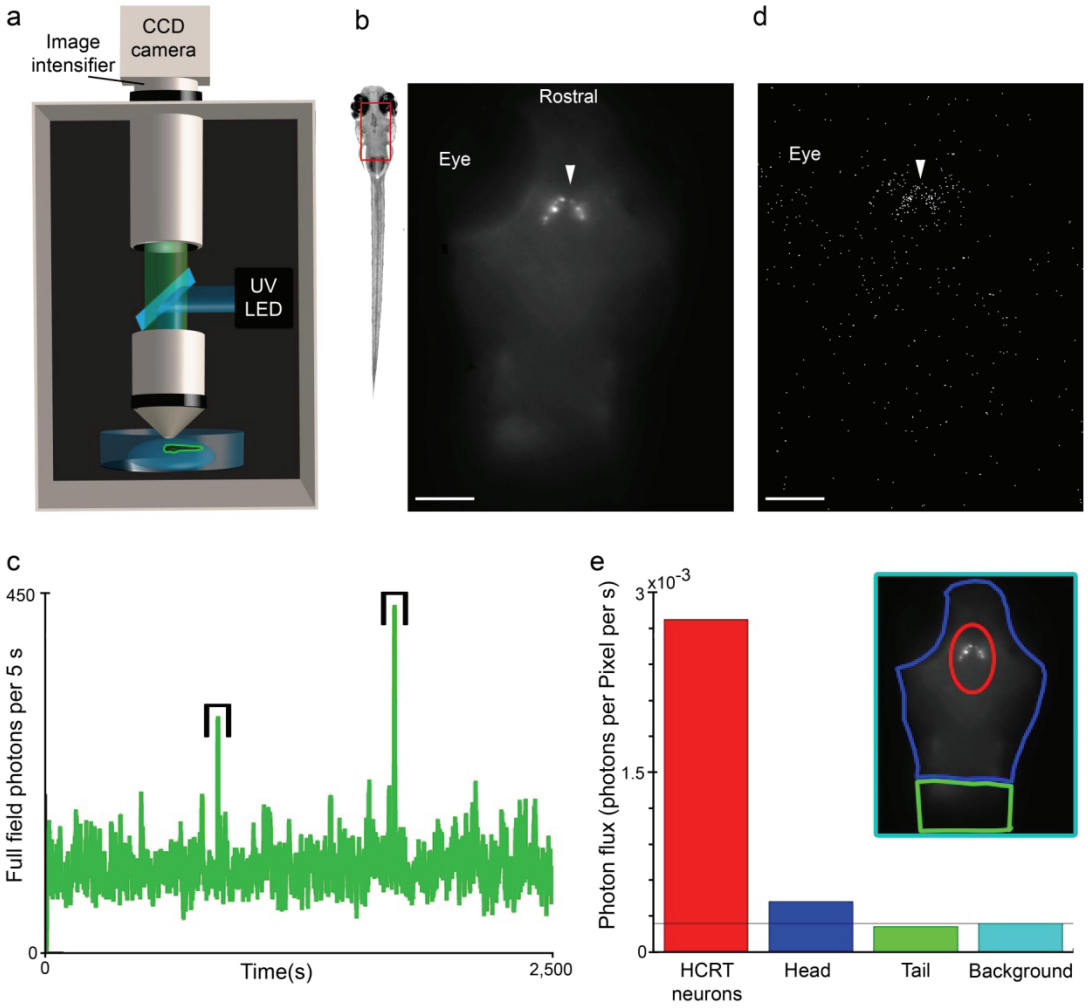

Supplementary Figure 11 – Photons are generated by GA-targeted HCRT neurons in restrained fish
a Schematic diagram of photon-counting imaging apparatus: an intensified CCD camera, custom epi-fluorescence microscope, and excitation light (UV LED) are assembled within a light tight enclosure. **b** A 5 dpf HCRT-GA larva was immobilized in low melting point agarose and the rectangle overlay indicates the region imaged to localize Aequorin expression via GFP fluorescence. The arrow indicates the HCRT somata (scale bar: 100 µm). **c** When epileptic-like neural activity is induced by the addition of PTZ (10 mM), transient increases in the total number of photons were observed . **d** The positional origin of the detected photons during these transient events is plotted. Also in a non-paralyzed zebrafish, the majority of photons arrive from the region containing the HCRT neurons; the arrow is located at the same position as in **b** (scale bar: 100 µm). **e** The photon flux (photons/pixel/second) from within four regions of interests (see inset): HCRT neurons, the imaged portion of the zebrafish head excluding the HCRT region, the rostral tail, and the background. Photon flux from the non-HCRT head region of the zebrafish is slightly above the background dark counts, which may represent photons originating from the axonal processes of the HCRT neurons (see **Figure 4**) or photons from HCRT neurons that are scattered within the fish body tissue.

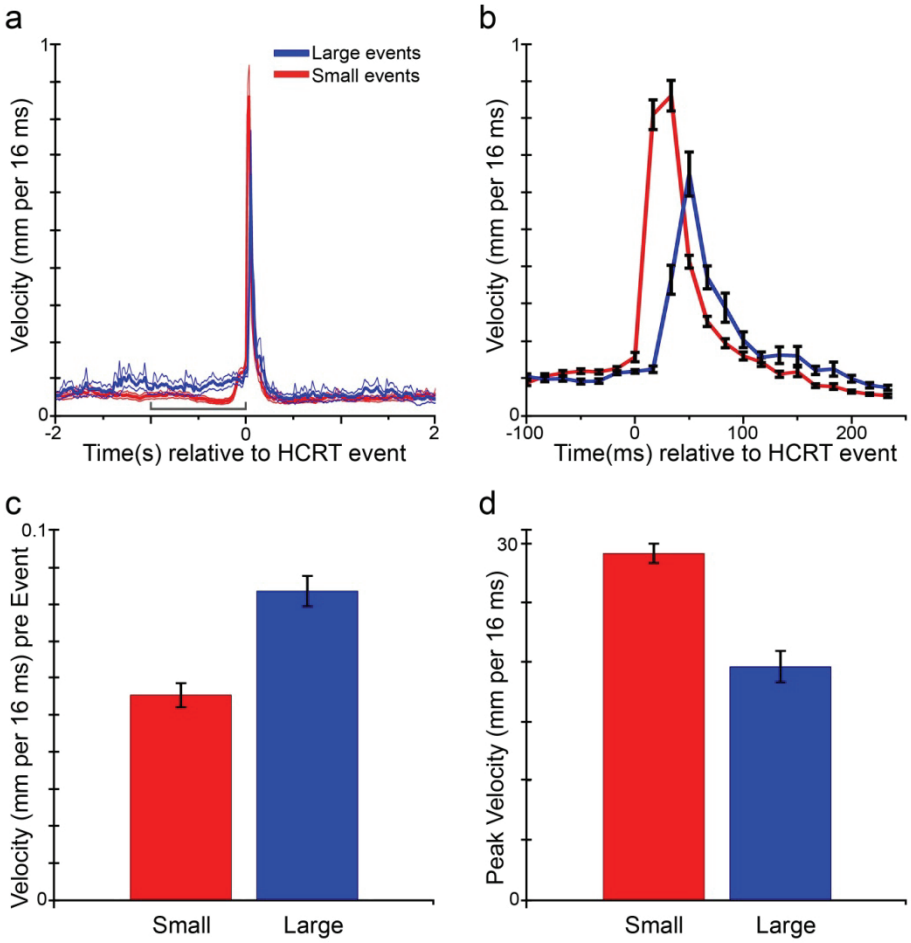

Supplementary Figure 12 –

Different amplitude signals from HCRT neurons are correlated with different behaviors

a The mean velocity of freely swimming HCRT:GA zebrafish in the two second time period surrounding large and small HCRT events (event time = 0 ms).The thin lines surrounding each mean plot demarcate a boundary of +/- 2 s.e.m. **b** An expansion of the time immediately surrounding the HCRT event. The difference in response latency for large and small HCRT events is apparent, as well as different velocity profiles (error bars represent s.e.m.). **c** Comparing the mean velocity within 1 second preceding the HCRT events (bracketed time region shown in **a**), demonstrates that zebrafish are more active prior to a large HCRT event than a small HCRT event. **d** Comparing the mean peak velocity reached following different HCRT events reveals that fish swim faster after a small HCRT event than after a large HCRT event (error bars represent s.e.m.).

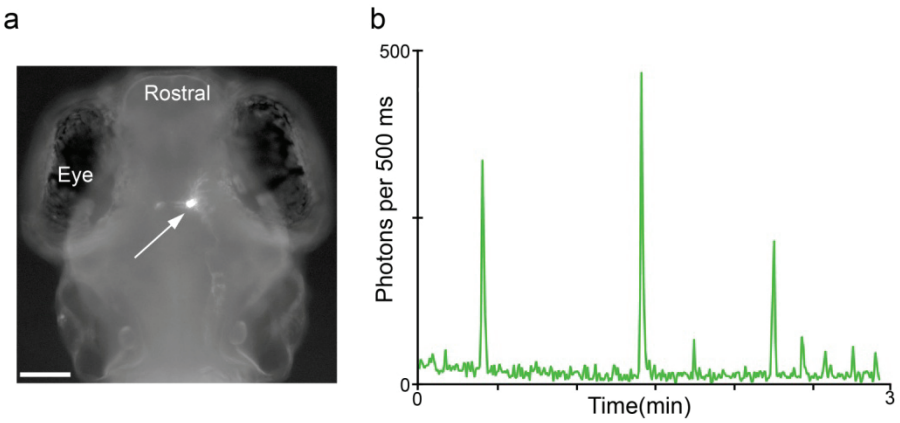

Supplementary Figure 13 – Neuroluminescence detection from single HCRT neurons

a Fluorescence micrograph of a zebrafish larva transiently expressing HCRT: Ga in a single neuron (soma indicated by arrow, scale bar: 100 µm). **b** Following constitution with CLZN for 24 hours, epileptic-like neural activity was induced by the addition of PTZ (10 mM), and large neuroluminescence signals were easily detected from an individual neuron in a freely moving animal.

Supplementary Movies

Supplementary Movie 1: Each panel displays a real-time movie (30 Hz) of a 7 dpf Nβt:GA zebrafish, previously exposed to CLZN for 24 hours, swimming freely in the neuroluminescence assay. In order to conveniently visualize neuroluminescence signals corresponding to behavior, the photons detected during each frame of the movie are plotted as green pixels in a disc surrounding the center of mass of the zebrafish image. Midway through the movie sequence, a mechanical stimulus is delivered by a computer-controlled tapping device. The stimulus time is indicated by a red circle appearing in the center of the movie frame.

Supplementary Movie 2: A neuroluminescence movie prepared similarly to that shown in Supplementary Movie 1, but displaying a zebrafish immediately (~1 minute) after exposure to PTZ.

Supplementary Movie 3: A neuroluminescence movie prepared similarly to that shown in Supplementary Movie 1, but displaying a zebrafish after prolonged exposure to PTZ (>20 minutes). Note that a brief initial swim bout is followed by a period without swimming that is corresponds with sustained neuroluminescence.

Supplementary Movie 4: A neuroluminescence movie prepared similarly to that shown in Supplementary Movie 1, but displaying a zebrafish paralyzed with α-Bungarotoxin and exposed to PTZ. The camera's zoom lens was used at full magnification, hence the reduced image quality, in order to assure that no motion was detected. Sporadic periods of sustained neuroluminescence are evident.

Supplementary Movie 5: The top row of panels display the average image acquired from a time series of two-photon images in three 5 dpf HuC:GCaMP2 zebrafish larva exposed to PTZ. The bottom row displays a movie (ten-fold accelerated) of the raw intensity images acquired during the time series. Long waves of correlated activity occur sporadically throughout the zebrafish brain.